ELSEVIER

Journal of Power Sources 76 (1998) 159–166

JOURNAL OF POWER SOURCES

Analysis of the surface of lithium in organic electrolyte by atomic force microscopy, Fourier transform infrared spectroscopy and scanning auger electron microscopy

Ken-ichi Morigaki *, Akira Ohta

Technology Laboratory, Matsushita Battery Industrial, 1, Matsushita-cho, Moriguchi, Osaka, 570-8511, Japan

Received 13 July 1998; accepted 22 August 1998

Abstract

The surface of lithium has been analyzed in a dry-air atmosphere and in 1 M $LiClO_4$/PC by in situ AFM observation and FTIR spectroscopy. High-resolution AFM discloses the nano-structure of the lithium surface which consists of grain boundaries, many ridge-lines, and flat areas. After immersing lithium in $LiClO_4$/PC, these lines swelled and large particles appeared. The surface chemistry of lithium has been examined by ex situ XPS and SAM. It is found that Li_2CO_3 and Li_2O localize on the ridge-lines and the grain boundaries. The morphological change due to lithium deposition occurs as a formation of particles on the ridge-lines and the grain boundaries.

Keywords: Lithium; Battery; AFM; FTIR; SAM; In situ analysis

1. Introduction

Lithium-ion batteries with anodes made from carbonaceous materials have recently been the subject of rapid development. It is highly expected that rechargeable lithium batteries using lithium metal anodes will offer higher specific energy. One of the difficulties in practical rechargeable lithium batteries is the low rechargeability of the lithium electrode, which is mainly due to the formation of lithium dendrites during the charging process. It appears, however, that the mechanism of lithium dendrite formation has not received sufficient research, and mere investigations of the surface structure of lithium are required.

The surface chemistry of lithium in organic electrolytes has been investigated indirectly with Fourier Transform Infrared (FTIR) spectroscopy by Aurbach et al. [1–8]. They also studied and compared the surface chemistry of graphite electrodes [9–13]. The results showed that solvents, such as propylene carbonate (PC), were decomposed on lithium and formed surface films of lithium alkylcarbonate, such as $ROCO_2Li$. In other studies, the lithium surface was investigated by ex situ X-ray photoelectron spectroscopy (XPS) [1,14–17], secondary ion mass spectroscopy (SIMS) [16] and scanning electron microscopy (SEM) [3,7,8]. It was found that the lithium surface consisted of Li_2CO_3, LiOH, Li_2O and lithium halides which were reduction products of the anion. Yamaki et al. [18,19] studied the factors which effect the cycling efficiency and the morphology of the lithium electrode, such as charging current density and pressure in the electrode stack.

In this study, we have investigated the surface chemistry of lithium in dry-air atmosphere and in 1 M $LiClO_4$/PC. In situ atomic force microscopy (AFM) and FTIR spectroscopy have been used to examine the nano-structure of the lithium surface and the interfacial reactions.

The surface chemistry of lithium has also been investigated by means of ex situ XPS analysis and scanning auger electron microscopy (SAM). The mechanism of

* Corresponding author. Tel.: +81-6-994-4552; Fax: +81-6-998-3179; E-mail: pan22005@pas.mbimei.co.jp

0378-7753/98/$19.00
PII: S0378-7753(98)00151-7

lithium deposition and the relationship to the surface morphology are discussed.

2. Experimental

Propylene Carbonate (PC) purchased from Mitsubishi Chemical and $LiClO_4$ purchased from Tomiyama Pure Chemical were used as received. The electrolyte was 1 M $LiClO_4$/PC with less than 50 ppm of water. Lithium foil purity = 99.9%, thickness = 0.18 mm) purchased from Kyokuto Metal served as the working electrode.

FTIR experiments were performed on a Mattson RS-2 spectrometer which was placed in a dry-air atmosphere which maintained a dew point of lower than −45°C. Double modulation FTIR (DMFTIR) spectroscopy [20–23] was performed using p-polarized and s-polarized IR beams modulated by a photoelastic modulator (PEM-90, Hinds) to investigate the surface chemistry of lithium. The DMFTIR spectra data are sampled by the real-time sampling electronics (Mattson) the difference between p-polarized data and s-polarized data as a sample spectrum, and the sum of p- and s-polarized data as a reference spectrum. The centre frequency of DMFTIR spectroscopy was set at 1200 cm^{-1}. One hundred scans were conducted in each measurement with a resolution of 2 cm^{-1}. The test cell was mounted on a NaCl optical window which had an angle of incidence of 70°. The optical system of DMFTIR measurement is the same as Reflection Absorption Spectroscopy (IRAS), and the system and the test cell have been described in a previous study [24].

AFM observations were performed by means of a TMX-1000, Topometrixs instrument which was also placed in the dry-air atmosphere. All AFM images were collected under conditions in which the probe contacted the lithium surface with a constant force. The AFM system and the structure of cell have also been reported in previous studies [25,26].

Chemical analysis of the lithium surface was performed with XPS-7000 (Rigaku) and SAM-670 (Ulvac Phi) instruments. The samples were immersed in electrolyte for 24 h and then washed with tetrahydrofuran (Tomiyama, purity: 99.9%) to remove electrolyte from the surface and dried in a dry-air atmosphere. The samples were set on holders in dry-air and transferred to the introduction chamber of the analysis equipment in a dry atmosphere. In depth-profile measurements, the lithium surface was sputtered by argon ions and the depth values were shown as in the case of SiO_2. The galvanostatic polarization for lithium deposition

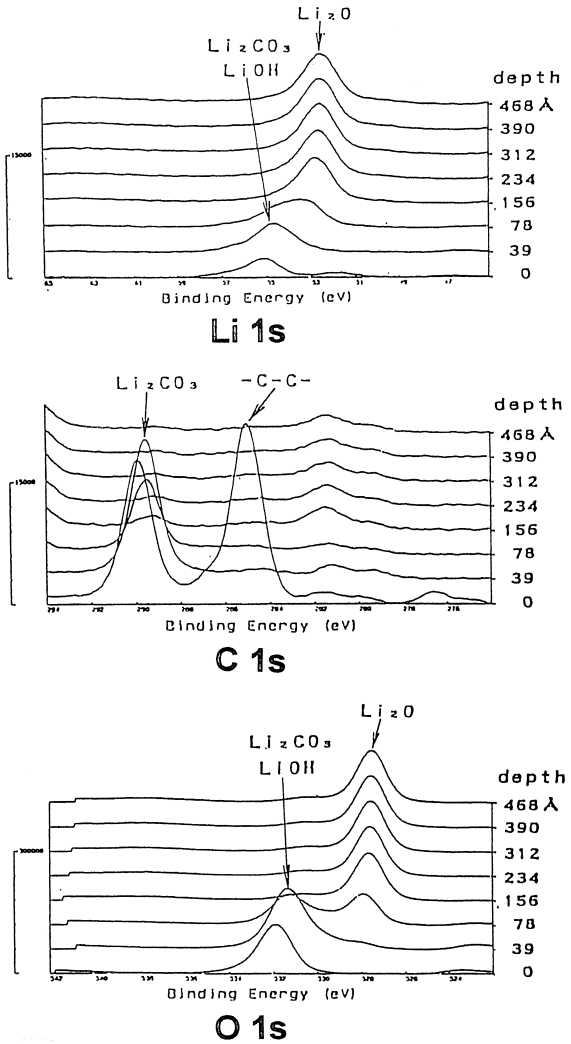

Fig. 2. XPS spectra of lithium with depth profile.

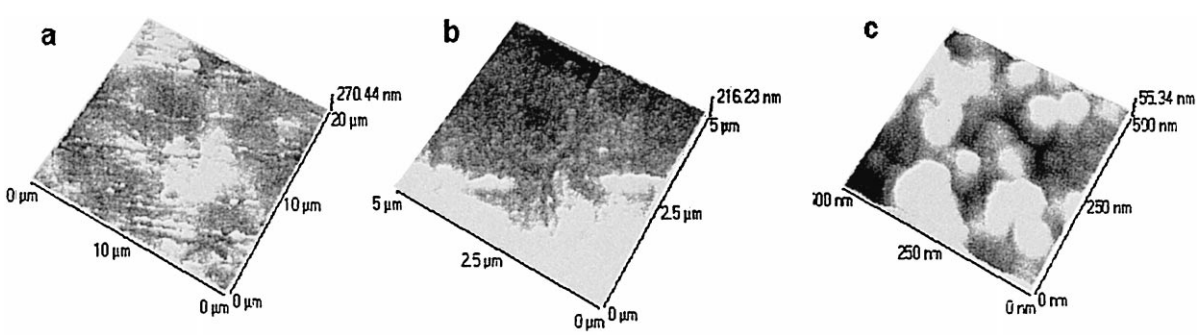

Fig. 1. AFM images of lithium surface: (a) 20 × 20 μm; (b) 5 × 5 μm; (c) 500 × 500 nm.

was performed by a potentio/galvanostat HA-301 (Hokuto denko). All experiments were performed at room temperature.

3. Results and discussion

AFM images of lithium are presented in Fig. 1. In the present study, AFM images are treated by a levelling process and a modification of the irregular traces in the scanning. The AFM images show that the lithium surface consists of grain boundaries, ridge-lines, and a flat area. The grain boundary is a columnar-like structure with a range of sizes from 1 to 2 μm. A ridge-line comprises stacks of elliptical grains with a range of sizes from 100 to 300 nm. On the other hand, the flat area which is surrounded by several ridge-lines is also stacks of elliptical grains with a range of sizes from 50 to 100 nm (Fig. 1(c)).

XPS spectra of the lithium surface and depth profiles are shown in Fig. 2. The O 1s, C 1s and Li 1s spectra indicate that Li_2CO_3 (O 1s: 531.5 eV, C 1s: 290 eV, Li 1s: 55.3 eV) exists on the surface and down to about 80 Å. The presence of LiOH (O 1s:531.5 eV, Li 1s: 55.3 eV) is not confirmed from these XPS spectra, although it was reported in the previous study [16] that LiOH can also exist in the film formed on the lithium surface. As the argon sputtering proceeded, new peaks were observed at 527.6 eV for O 1s and at 53 eV for Li 1s spectra, which were assigned to Li_2O. These results are consistent with those of previous XPS studies [13,15,16].

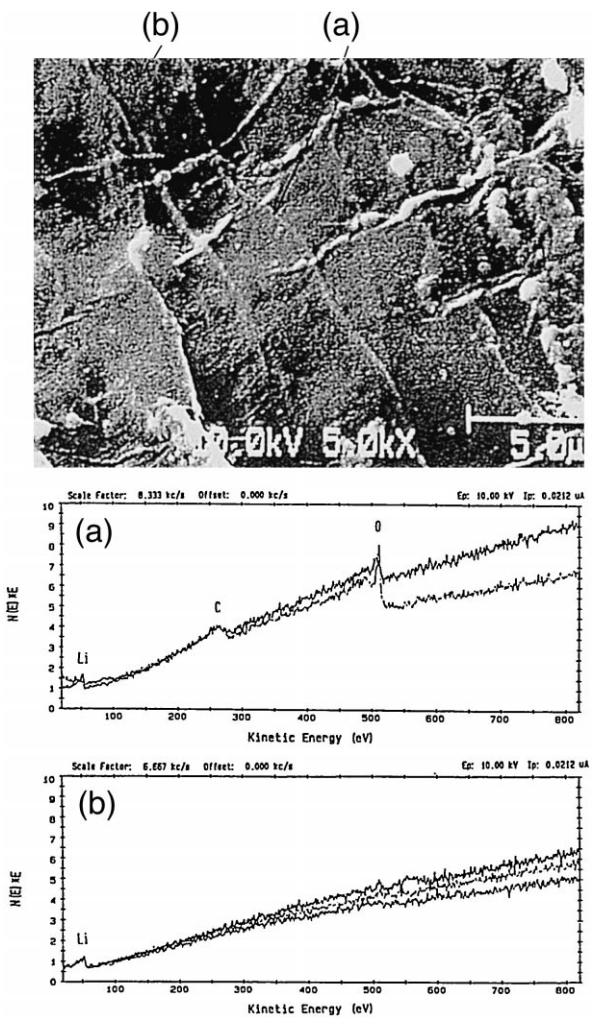

Fig. 3. SEM image and AES spectra of lithium: (a) line; (b) flat area.

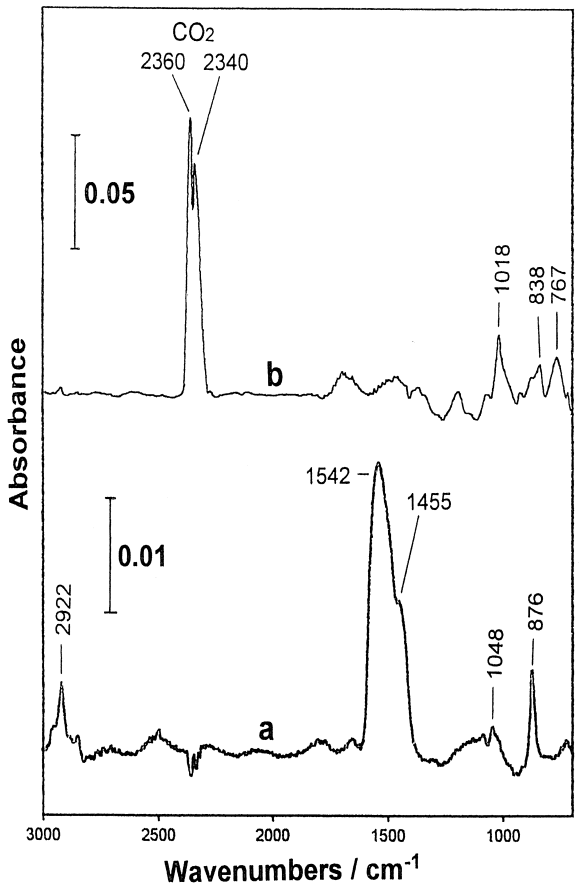

Fig. 4. Comparison of IRAS and DMFTIR spectra of lithium surface: (a) DMFTIR spectrum; (b) IRAS spectrum.

A scanning electron micrograph and AES spectra for lithium with depth profiles are given in Fig. 3. The locations used to obtain the AES spectra are shown in the micrograph. It is found that O and C are localized on the ridge-lines and the grain boundaries (Fig. 3(a)), while only Li is observed in the flat-area (Fig. 3(b)). Therefore, it is concluded that Li_2O, Li_2CO_3 and LiOH exist in the ridge-lines and the grain boundaries. Also, non-uniform native films are formed on the lithium surface as proposed before [16,17], but the localized distribution of surface species exists on the lithium surface the same manner as the morphology.

A comparison between the DMFTIR spectrum and the IRAS spectrum of the lithium surface in the dry-air atmo-

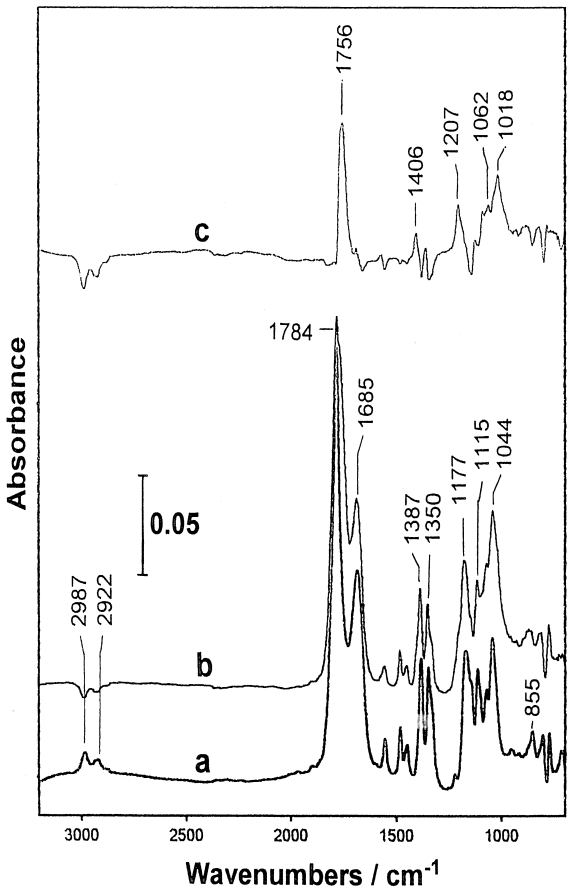

Fig. 5. DMFTIR spectra of PC and $LiClO_4$/PC solution: (a) PC; (b) $LiClO_4$/PC; (c) subtractive spectrum.

sphere is shown in Fig. 4. The IRAS spectrum of the lithium surface was obtained by using the spectrum of a copper surface as a reference. The DMFTIR spectrum showed the peaks due to Li_2CO_3 are at 876 and around 1542 to 1455 cm^{-1}, which is consistent with the peaks reported in previous studies [1–12]. The peaks due to LiOH (around 3660–3675 cm^{-1}) [1,2] are not observed clearly, however, and the small peaks around 1050 and 2920 cm^{-1} reveal the presence of an organic compound on the lithium surface. The IRAS spectrum has major peaks at 2360 and 2340 cm^{-1}, which are characteristic doublet peaks of CO_2. The other peaks from 1018 to 767 cm^{-1} indicate the presence of an organic compound, but the peaks corresponding to Li_2CO_3 are not observed clearly in the IRAS spectrum. From these results, we conclude that DMFTIR spectra can provide information about phenomena on the surface, while IRAS spectra provide information about phenomena both in the bulk and on the surface.

The DMFTIR spectra of solvent (PC) and electrolyte (1 M $LiClO_4$/PC) on lithium are shown in Fig. 5(a) and (b), respectively. The difference in the spectra is shown as the subtractive spectrum in Fig. 5(c). The major peak of the spectra is observed at 1782 cm^{-1}, which is ascribed to the C=O stretching vibration ($\upsilon_{C=O}$) of PC. The peaks around 1685, 1350, 1115, 1044 and 855 cm^{-1} are ascribed to lithium alkylcarbonate as reported in previous studies [1–5,7], in which the reduction product of PC had peaks at 1690–1640 ($\upsilon_{AS,\,C=O}$), 1450–1400 (δ_{CH}), 1350–1320 ($\upsilon_{S,\,C=O}$), 1100–1060 (υ_{C-O}), and 820 (δ_{CO3}) cm^{-1}. The subtractive spectrum in Fig. 5(c) shows the changes in the interface caused by the dissolution of $LiClO_4$. The major peak is observed at 1756 cm^{-1}, which is also ascribed to the C=O stretching vibration ($\upsilon_{C=O}$) of lithium alkylcarbonate ($ROCO_2Li$). The peak at 1062 cm^{-1} is the characteristic peak of electrolytes which contain $LiClO_4$, while the other peaks at 1207 and 1018 cm^{-1} correspond to the solvation of Li^+ ion or $ROCO_2Li$.

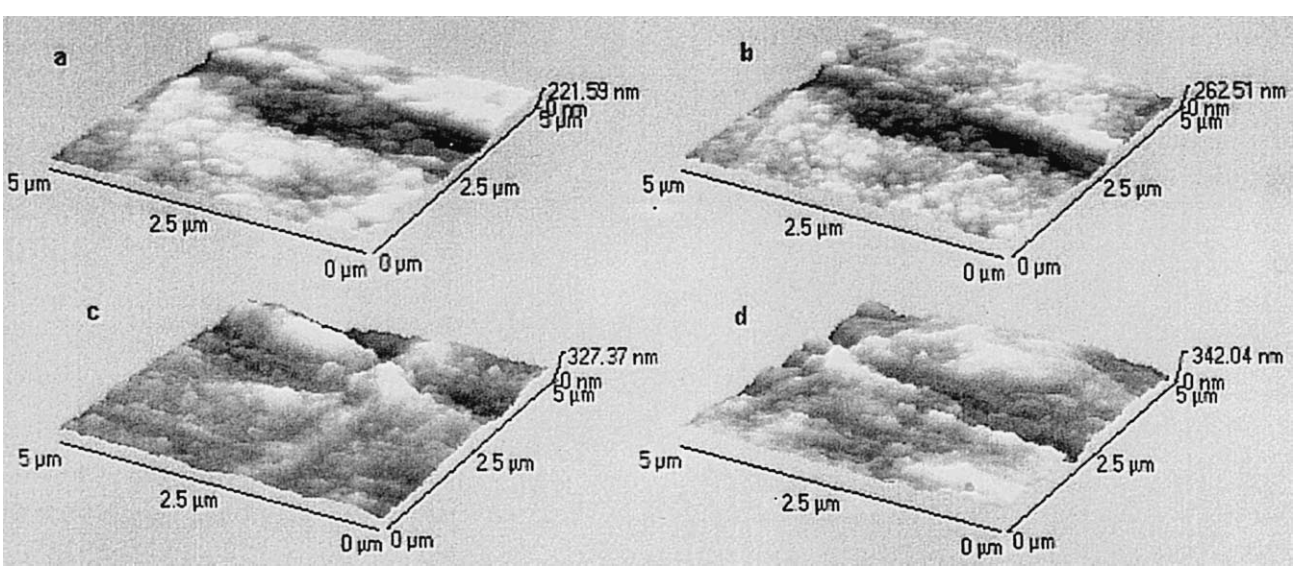

Fig. 6. AFM images of lithium in 1 M $LiClO_4$/PC: (a) initial state; (b) after 3 h; (c) 15 h; (d) 24 h.

The morphological changes in lithium after immersion in 1 M $LiClO_4$/PC, as detected by AFM measurement, are presented in Fig. 6. The lithium surface is shown to be a stack of small particles (300-600 nm in size) in the electrolyte at the initial state (Fig. 6(a)). The lithium surface is covered by many smaller particles (about 100 nm in size) after the immersion in the electrolyte. It appears that the solvent (PC) is reduced to lithium alkylcarbonate ($ROCO_2Li$) and the latter causes the formation of these particles on the lithium surface. After immersion for 24 h, the ridge-lines and the grain boundaries swell to over 100 nm, and several particles in the size range 500 to 1000 nm are observed on these lines. We conclude that these morphological changes are related to a difference in the surface reaction, that is, the reduction of solvent or salt on these lines is different from the reaction on the flat areas.

Changes in the DMFTIR spectra with immersion time in 1 M $LiClO_4$/PC are given in Fig. 7. The peak at 1784 cm^{-1} due to PC($\upsilon_{C=O}$), remains as the major peak, even after 24 h. The peak around 1680 cm^{-1} which is ascribed to $ROCO_2Li$, increases with immersion time. The other peaks exhibit little change with immersion time.

A comparison between the DMFTIR spectra of $LiClO_4$/PC in the initial state and after immersion for 24 h is shown in Fig. 8. The subtractive spectrum (Fig. 8(c)) displays some increasing peaks at 1663 ($\upsilon_{C=O}$), 1387, 1350 (δ_{CH}), 1164, 1070 (υ_{C-O}), and 876 cm^{-1}. The peak at 876 cm^{-1} is ascribed to δ_{OCO_2} of Li_2CO_3 (see Fig. 4(a)), but the peaks at 1542 and 1455 cm^{-1} of Li_2CO_3 are hidden by solvent peaks. The other peaks from 1663 to 1070 cm^{-1} are ascribed to lithium alkylcarbonate ($ROCO_2Li$), which is a reduction product of PC.

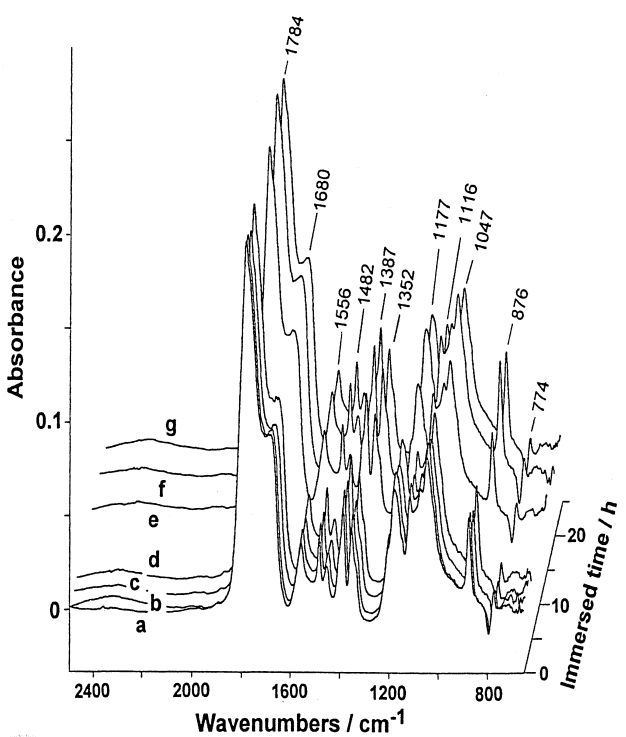

Fig. 7. Changes of DMFTIR spectra of $LiClO_4$/PC on lithium with immersed time. (a) 0 h; (b) 1 h; (c) 3 h; (d) 5 h; (e) 15 h; (f) 20 h; (g) 24 h.

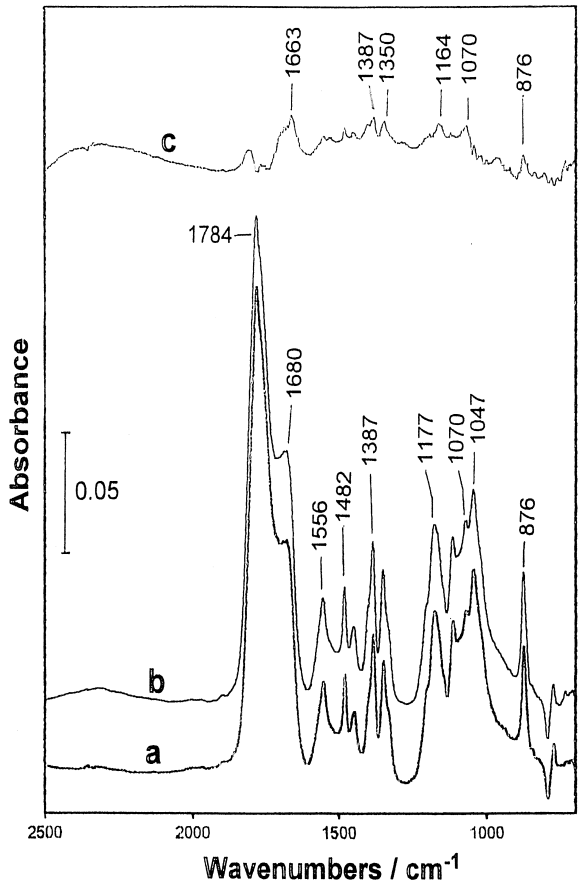

Fig. 8. DMFTIR spectra of 1 M $LiClO_4$/PC on lithium in initial state and after 24 h: (a) initial state; (b) after 24 h; (c) subtractive spectrum.

The XPS spectra of the lithium surface after immersion in the electrolyte for 24 h are presented in Fig. 9. It is observed that the ClO_4^- anion is absorbed on the lithium surface, to give a peak at 209 eV for Cl 2p spectra, and reacts with lithium to form LiCl, with a peak at 198.4 eV, in the inner layer. This result is consistent with a previous XPS study [13]. New peaks are observed at 533.8 eV for O 1s and 290.6 eV for C 1s, and which is ascribed to $-OCO_2-$, and the peak at 287 eV for C 1s is ascribed to –C–O– on the surface. These peaks disappear during argon sputtering to a depth of about 40 Å. Therefore, this thought that PC is absorbed and reduced to form $ROCO_2Li$ all over the lithium surface. On the other hand, the peaks assigned to Li_2O (or LiOH) and Li_2CO_3 change little after immersion in the electrolyte.

A scanning electron micrograph and AES spectra of lithium after immersion in the electrolyte are shown in Fig. 10 with depth profiles. It is found that Cl exists on the ridge-lines and the grain boundaries in both surface spectra

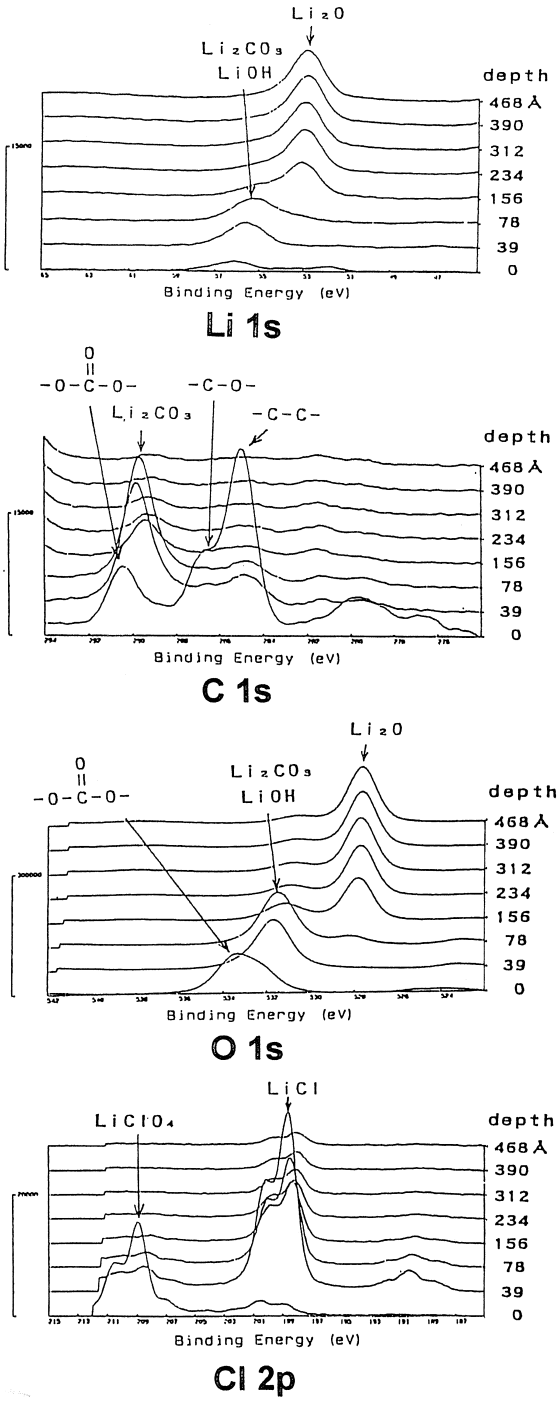

Fig. 9. XPS spectra of lithium after immersion in $LiClO_4$/PC for 24 h with depth profiles.

and depth-profiling spectra, but no peak assigned to Cl is observed on the flat area. The AES spectra reveal that O and C exist on the flat area, and which means that PC is absorbed and reacts on the flat area. The AES spectra from the ridge-lines, except Cl, are similar to the spectra from the flat areas. Therefore, it is considered that the ClO_4^- anion reacts with lithium to form LiCl on the ridge-lines and the grain boundaries, and the reduction of ClO_4^- to form LiCl on these lines causes the large expansion of these lines. On the other hand, the solvent (PC) is absorbed and reduced to form $ROCO_2Li$ all over the lithium surface.

Fig. 11 resents AFM images of lithium deposited on lithium in $LiClO_4$/PC with line profiles. The current density of deposition was 2 mA cm^{-2}, and the amount of deposition was 0.36 C cm^{-2}. Many particles of deposited lithium are observed on the ridge-lines and the grain boundaries. The typical size of the particle is about 400 nm in length and about 100 nm in height, and the largest one is 700 nm in length and 200 nm in height. The line profiles (Fig. 11(c) and (f)) show that some of the surface morphology remains unchanged after deposition. It appears that the change in morphology due to deposition is raised from the baseline of lithium surface. Therefore, in order to understand this phenomenon, we propose that the growth of lithium in electrodeposition occurs mainly by bulk diffu-

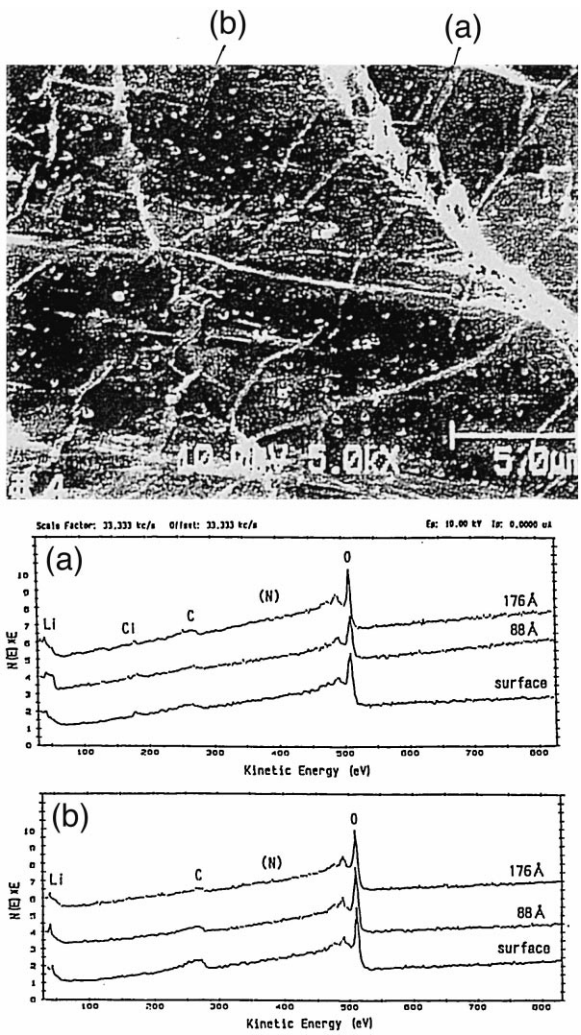

Fig. 10. SEM image and AES spectra of lithium after immersion in $LiClO_4$/PC for 24 h with depth profiles. SEM image obtained at 88 Å: (a) line; (b) flat area.

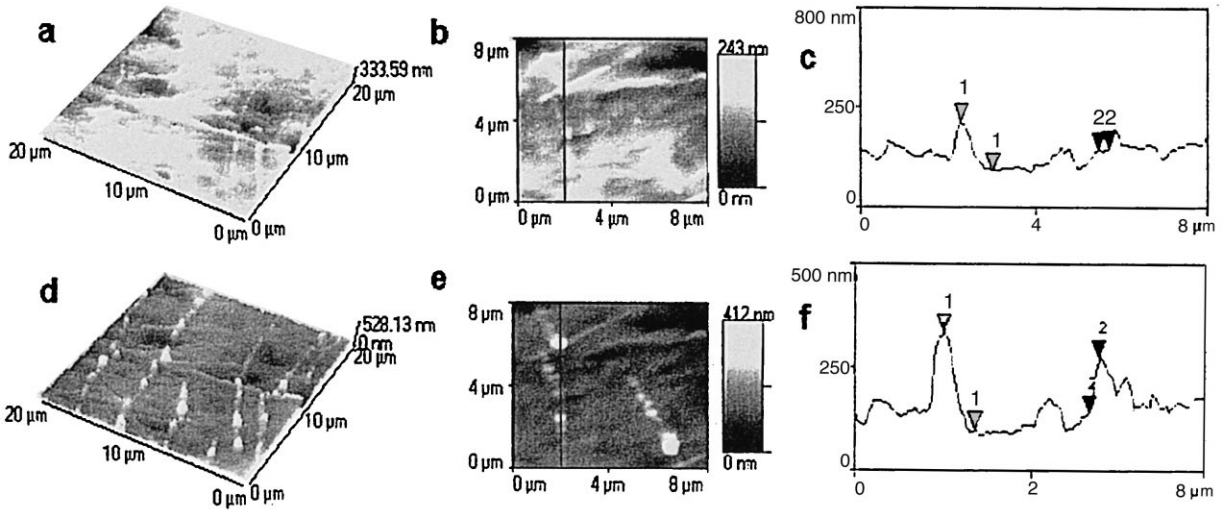

Fig. 11. AFM images of lithium deposited on lithium electrode in 1 M in $LiClO_4$/PC with line profiles: (a)–(c) before deposition; (d)–(f) deposited lithium at 2 mA cm^{-2}, 0.36 C cm^{-2}; (a) and (d) 3D images (20×20 μm); (b) and (e) top views (8×8 μm); (c) and (f) line profiles of (b) and (e).

sion and not by surface diffusion. We suggest that there may be many dislocations and defects in the grain boundaries and scratches during processing, and O_2, CO_2 and H_2O in the atmosphere react to form Li_2CO_3 and Li_2O [27,28] at these active sites. Thus, the scratches are raised as ridge-lines containing high porosity and many active sites. Since the flat areas are covered with solvent (PC) and reduction product ($ROCO_2Li$), Li^+ ions and even counter anions ($ClO4^-$) migrate through the ridge-lines and the grain boundaries. During electrodeposition, the migration of Li^+ ions occurs through the ridge-lines and the grain boundaries through bulk diffusion. At a high current density, such as 2 mA cm^{-2}, lithium deposition occurs on the ridge-lines and the grain boundaries, (Fig. 11(d) and (e)) because the rate of bulk diffusion is slower than that of migration.

4. Conclusions

The present study has proved that in situ AFM observation and in situ DMFTIR spectroscopy are effective techniques for the analysis of the lithium surface, even in organic electrolyte. It is shown that DMFTIR spectroscopy is an effective detection method of the surface chemistry and the interfacial reactions. Examination by AFM and SAM has revealed a new structure of lithium. The structure of the lithium surface consists of grain boundaries, ridge-lines, and flat areas. The grain boundary and the ridge-line which consist of Li_2CO_3, Li_2O and the reduction products of the electrolyte (such as LiCl) have dislocations and defects. We propose that the morphological changes due to deposition of lithium are caused by bulk diffusion through the ridge-line and the grain boundary. Consequently, it is concluded that these lines are very important factors in controlling the morphology of deposition, such as dendrite formation.

Acknowledgements

The authors are grateful to the New Energy and Industrial Technology Development Organization for supporting this work.

References

[1] D. Aurbach, M.L. Daroux, P. Faguy, E.B. Yeager, J. Electrochem. Soc. 134 (1987) 1611.
[2] E. Goren, O.Y. Chusid, D. Aurbach, J. Electrochem. Soc. 138 (1991) L6.
[3] D. Aurbach, Y. Gofer, J. Electrochem. Soc. 138 (1991) 3529.
[4] D. Aurbach, Y. Gofer, M. Ben-Zion, P. Aped, J. Electroanal. Chem. 339 (1992) 451.
[5] D. Aurbach, O.Y. Chusid, J. Electrochem. Soc. 140 (1993) L155.
[6] D. Aurbach, Y. Ein-Eli, A. Zaban, J. Electrochem. Soc. 141 (1994) L1.
[7] D. Aurbach, I. Weissman, A. Zaban, O.Y. Chusid, Electrochim. Acta 39 (1994) 51.
[8] D. Aurbach, A. Zaban, A. Shechter, Y. Ein-Eli, E. Zinigrad, B. Markovsky, J. Electrochem. Soc. 142 (1995) 2873.
[9] D. Aurbach, O.Y. Chusid, Y. Carmeli, M. Babai, Y. Ein-Eli, J. Power Sources 43–44 (1993) 47.
[10] D. Aurbach, Y. Ein-Eli, O. Chusid, M. Babai, Y. Cameli, H. Yamin, J. Electrochem. Soc. 141 (1994) 603.
[11] D. Aurbach, Y. Ein-Eli, B. Markovsky, A. Zaban, S. Luski, Y. Carmeli, H. Yamin, J. Electrochem. Soc. 142 (1995) 2882.
[12] D. Aurbach, B. Markovsky, A. Shechter, Y. Ein-Eli, H. Cohen, J. Electrochem. Soc. 143 (1996) 3809.
[13] Y. Ein-Eli, S.R. Thomas, V. Koch, D. Aurbach, B. Markovsky, A. Schechter, J. Electrochem. Soc. 143 (1996) L273.
[14] G. Nazri, R.H. Muller, J. Electrochem. Soc. 132 (1985) 2050.
[15] N. Kasahara, H. Nishihama, J. Power Sources 20 (1987) 265.

[16] K. Kanamura, H. Tamura, Z. Takehara, J. Electroanal. Chem. 333 (1992) 127.
[17] K. Kanamura, S. Shiraishi, H. Tamura, Z. Takehara, J. Electrochem. Soc. 141 (1994) 2379.
[18] M. Arakawa, S. Tobishima, Y. Nemoto, M. Ichimura, J. Yamaki, J. Power Sources 43–44 (1993) 27.
[19] T. Hirai, I. Yoshimatsu, J. Yamaki, J. Electrochem. Soc. 141 (1994) 611.
[20] K. Kunimatsu, H. Kita, J. Electroanal. Chem. 218 (1987) 155.
[21] B.J. Barner, M.J. Green, E.I. Saez, R.M. Corn, Anal. Chem. 63 (1991) 55.
[22] B.L. Frey, D.G. Hanken, R.M. Corn, Langmuir 9 (1993) 1815.
[23] E.I. Saez, R.M. Corn, Electrochim. Acta. 38 (1993) 1619.
[24] K. Morigaki, T. Fujii, A. Ohta, Extended Abstracts of the 37th Battery Symposium, Tokyo, Japan, 1996, p. 167.
[25] K. Morigaki, N. Kabuto, K. Yoshino, A. Ohta, Extended Abstracts of the 35th Battery Symposium, Nagoya, Japan, 1994, p. 83.
[26] K. Morigaki, N. Kabuto, K. Yoshino, A. Ohta, Power Sources 15, in: A. Attewell, T. Keily, (Eds.), Int. Power Sources Symposium Committee, 1995, p. 267.
[27] K. Wang, P.N. Ross Jr., F. Kong, F. McLarnon, J. Electrochem. Soc. 143 (1996) 422.
[28] G. Zhuang, P.N. Ross Jr., F. Kong, F. McLarnon, J. Electrochem. Soc. 145 (1998) 159.